Available online at www.sciencedirect.com

ScienceDirect

Procedia Structural Integrity 28 (2020) 1276–1285

Structural Integrity Procedia

www.elsevier.com/locate/procedia

1st Virtual European Conference on Fracture

A new analytical model to estimate maximum internal socket depth of non-reduced strength bolts

Fatih Kocatürk[a,b], M. Burak Toparli[a], Barış Tanrıkulu[a,c], Umut İnce[a], Cenk Kılıçaslan[a,*]

[a]*Norm Cıvata R&D Center, Norm Cıvata San. ve Tic. A.Ş., A.O.S.B., Çiğli, İzmir, Turkey*
[b]*Graduate School, Applied Mathematics and Statistics, İzmir University of Economics, İzmir, Turkey*
[c]*The Graduate School of Natural and Applied Sciences, Dokuz Eylül University, İzmir, Turkey*

Abstract

In this study, an analytical model for calculation of the maximum socket depth of bolts having shaft diameter smaller than socket diameter was introduced. A representative bolt was chosen and maximum socket depth satisfying the minimum ultimate tensile strength was calculated by the developed analytical model. The analytical findings were also compared with numerical simulations for validation. Numerical studies were carried out by using Simufact.forming finite element software. The maximum socket depth estimated by using the developed analytical model was in good agreement with the numerical results. The obtained critical socket depth through the analytical model was 1.4% safer compared to numerical simulation results. Therefore, it was concluded that the developed analytical model could be used to estimate the critical socket depths of bolts having shaft diameter smaller than socket diameter.

Keywords: Fracture (mathematical); Failure criterion; Structural integrity; Mechanical testing; Finite element modelling; Metal forming; Industrial applications

1. Introduction

Bolts, or fasteners, are one of most widely used engineering products used to assemble two or more components. Depending on the application, bolts are produced in various size, shape and grade which are effective on the

* Corresponding author. Tel.: +90-232-376-7610; fax: +90-232-376-7613.
E-mail address: cenk.kilicaslan@norm-fasteners.com.tr

2452-3216
10.1016/j.prostr.2020.11.109

mechanical behaviour. Considering service conditions, the factors that have to be considered in evaluating the strength of a threaded fastener were explained in (Bickford, 1998). Tensile loading, shear loading, torsional loading as well as combined loading were analysed in detail for threaded fasteners.

Nomenclature

α	the angle under the line passing through the end of socket and tip of socket
φ	the angle formed between the fracture pattern and the vertical line passing from point p
τ_B	the torsional strength
A_S	the nominal cross sectional area of the bolt thread
A_{Sch}	the surface area of the fracture cone formed in the head
d_m	the minimum socket diameter
d_{Sch}	the shaft diameter
f	difference between d_{Sch} and d_m
l_i	the equation of the i^{th} line
m	slope of a line
m_i	the slope of the i^{th} line
R	the radius of the head
R_m	the tensile strength
R_{mred}	the resultant of the tensile stress ($R_m.\sin\varphi$) and the shear stress ($\tau_B.\cos\varphi$) acting on the fracture cone
t	sum of d_{Sch} and d_m
x	apsis of the fracture point p
x^*	the strength ratio
y	ordinate of the fracture point p
y^*	sum of y_{min} and the radius R
y_{min}	the minimum distance between the end of the socket and the bottom of the head

In addition to loading conditions, there are different features of fasteners having strong impact on failure mechanism and service life. For instance, the effect of socket depth on failure types of fasteners was investigated in (Tanrıkulu et al., 2018). In this study, experimental studies on cold forged bolts having various socket depths were carried out and torque-tension tests were conducted to reveal the effects of critical socket depth under different loading types. It was observed that the socket depth has significant influence on failure mechanism of fasteners. M8x1.25x50 Full Thread (FT) bolts with 10.9 and 8.8 grade were examined to determine the effect of socket depth for the purpose of weight reduction in (Tanrıkulu et al., 2019), as a continuation of the study of (Tanrıkulu et al., 2018). In order to determine the critical socket depth; i.e. the highest weight reduction, Finite Element (FE) simulations and experimental torque-tension tests were performed for the type of fastener being investigated. One of the analytical models used to estimate socket depth introduced in the literature by (Thomala and Kloos, 2007) was also used to compare the results obtained from numerical and empirical studies.

There exist studies concerning the failure modes of bolt and nut assemblies in the literature. The failure modes of bolt and nut assemblies under tension can be divided into three groups: bolt fracture, bolt thread failure, and nut thread failure. Using partially threaded bolt rather than fully threaded in connections could increase the possibility of thread failure (Grimsmo et al., 2016). Thread failure of the bolt-nut assemblies subjected to tension is generally undesirable since it is a less ductile failure mode than the bolt fracture (fracture of the threaded shaft of the bolt). Therefore, investigation of the causes of thread failure is important and the effect of the length of the threaded bolt shaft located within the grip was examined in (Grimsmo et al., 2016). The fatigue damage assessments of the M10 bolted joint made of 42CrMo4 heat treatable steel and grade 10.9 were performed in (Novoselac et al., 2014) for variable preload forces and variable amplitude eccentric forces for high reliability. Preload forces of 0%, 50%, 70% and 90% of force at bolt yield point were used to make assessments. In order to define the material cyclic scatter band having Gaussian normal distribution in logarithmic scales, range of dispersion was used. The multiaxial fatigue stress criterion based on a

critical plane theory for fatigue damage assessment was applied to obtain the multiaxial stress field with high notch effect in thread root. The critical plane approach was used to estimate fatigue damage and fatigue fracture plane position. The fatigue life of the bolts is usually calculated using the nominal approach applied under normal loads, but this method is insufficient for multiaxial loads. To this end, an effective method for calculating fatigue-induced damage to bolts was developed by improving the Schneider's method (Sorg et al., 2017).

Experimental studies to investigate the mechanical performance of high-strength 8.8 grade bolts under tensile load were conducted in (Hu et al., 2016). As a result of tests, it was observed that the failure of structural bolts occurred in two different ways: stripping on the thread and necking in the threaded portion of the bolt shaft. The fracture behaviour of 42CrMo ultrahigh strength steel-based bolt was investigated experimentally in (Hongfei et al., 2019) by performing macroscopic and microscopic fracture observation, metallographic test, mechanical property test and energy spectrum analysis. The results showed that a large amount of structural defect, such as sulphur inclusions, band and carbon depletion, appears in the fracture origin region and matrix of the bolt. Such defects reduced the fatigue strength of materials and led to fatigue failures. In the study performed by (Hedayat et al., 2017) for the prediction of bolt fracture in shear when threads are excluded from the shear plane, finite element methods were divided into two main categories in order to determine the appropriate failure criteria: i) Monitoring the level of stress and strain at the critical elements of the bolt shaft, ii) Describing crack initiation and crack formation.

The tensile state of bolts and nuts with ISO metric thread design was examined and optimized in (Pedersen, 2013). The maximum tension in the bolt was located in the fillet under the head, at the beginning of the thread or at the thread root. To minimize the stress concentration, shape optimization was applied. In this context, first the fillet under the head, nut thread design and the fillet in the shaft and thread transition region were optimized and 25.3%, 15.8% and 34% stress reductions were achieved, respectively. These design improvements, which lead to the reduction of stress in the bolt, was also observed to reduce the hardness of the bolt. Threaded fasteners are expected to fracture from the thread region under service loads. (ISO 898-1, 2004) standard dictates certain tensile strengths and bolts are expected to fracture from the thread region. The depth of the internal socket form at head of bolts is very crucial since it is one of the most important design parameters affecting the structural integrity of bolts, i.e. depending on the depth, the failure mode of bolts can mitigate from thread root to under head region. However, in some cases, it is known that the bolts are also fractured from the head region due to the bolt design required for specific applications, and this type of bolts must satisfy the minimum ultimate tensile strength given in (ISO 898-1, 2004) under tension loading.

Considering failure mechanisms of the bolts, the fracture cone formed under the bottom of the socket and the under head region was analysed in (Thomala and Kloos, 2007) for the bolts having shaft diameter larger than socket diameter. An analytical model was introduced to calculate the minimum height between the bottom of the socket and the head, i.e. the socket depth. The proposed model is valid for the case shaft diameter is greater than or equal to the socket diameter of the bolts with internal socket form. Eq. (1) was derived by (Thomala and Kloos, 2007) and referenced in VDI 2230 standard to estimate critical socket depth for bolts having shaft diameter greater than the socket diameter:

$$y_{min} = \frac{\sqrt{16A_S^2 - \pi^2\left(d_{Sch}^2 - d_m^2\right)^2}}{2.x^*.\pi.(d_{Sch}+d_m)} \tag{1}$$

where A_S is the nominal shaft cross-sectional area, d_{Sch} is the shaft diameter, d_m is the average socket diameter, $x^* = \frac{\tau_B}{R_m}$ is the strength ratio and τ_B is the torsional strength, R_m is the tensile strength (see Fig. 1).

In addition to bolt type investigated in Eq. (1), bolts having shaft diameter smaller than socket diameter are also preferred for certain applications, and there was no study in the literature on this type of bolts. In this study, analytical and numerical works were carried out on bolts having shaft diameter smaller than socket diameter. An analytical model was developed to estimate the maximum socket depth of bolts having shaft diameter smaller than socket diameter. For the sake of validation, a representative bolt geometry was chosen and FE model was constructed to compare the critical socket depth estimated by the analytical model.

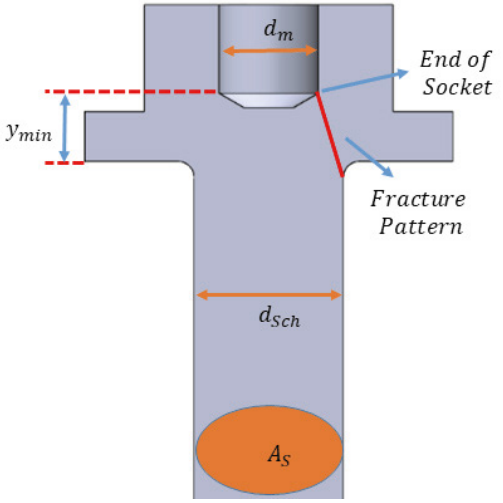

Fig. 1. Schematic of bolt having shaft diameter greater than the socket diameter.

2. Sample specification

In this study, M8 bolt with 1,25 thread pitch and 23 mm shaft length was chosen as the representative sample. Bolt with N10 socket form and satisfying the mechanical requirements for 8.8 grade as given in (ISO 898-1, 2004) was modelled by using Simufact.forming finite element software. The material was 23MnB4, i.e. one of the most widely preferred low alloy steel in cold forging.

3. Socket depth estimation for bolts having shaft diameter smaller than socket diameter

3.1. Analytical modelling

Analytical Modelling studies were initiated by investigating Eq. (1) in detail, which is valid for the case of bolts having shaft diameter greater than the socket diameter. The minimum distance between the end of the socket and the bottom of the head, y_{min}, can be found in Eq. (1). The y_{min} value is called as the residual floor thickness and measured with the relation $y_{min} = k - s$ for an inbus bolt where the head height is k and the socket depth is s shown in Fig. 2.

When the shaft diameter is greater than the socket diameter, the fracture pattern is expected to be formed between the bottom of head and the end of the socket (see Fig. 1). However, when the shaft diameter is smaller than the socket diameter, the fracture pattern was formed between the bottom of head and a point p, which is located between the end of the socket and the tip of the socket based on the experiences in production (see Fig. 2).

The two-dimensional bolt cross section is shown in Fig. 3 to locate the break point, p_1, required to calculate the surface area of the fracture cone. The local origin of the cross sectional area, $(0,0)$ is selected as shown in Fig. 4. Then, $p_1 = (x, y)$ is obtained as follows:

Let us call the line passing through p_1 and p_2 as l_1 and the line passing through p_1 and p_3 as l_2.

- First, the equation of the line l_1 is found by using the slope of the line, $m_1 = \tan\alpha$, and the point $p_2 = (\frac{d_m}{2}, y_{min} + R)$ in Eq. (3). The equation of a line can be found given that a point, $A = (x_0, y_0)$, on the line and its slope, m, is known by using Eq. (2).

$$y - y_0 = m.(x - x_0) \tag{2}$$

If $m = m_1$ and $A = p_2$ are put in Eq. (3), the equation of the line l_1 in Eq. (4) is obtained.

$$y = \tan\alpha \,.\left(x - \frac{d_m}{2}\right) + (y_{min} + R) \tag{3}$$

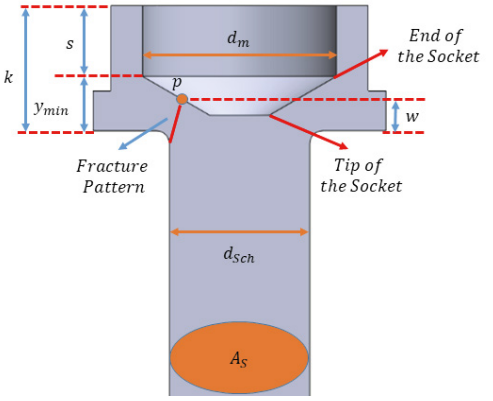

Fig. 2. Schematic of bolt having shaft diameter smaller than the socket diameter.

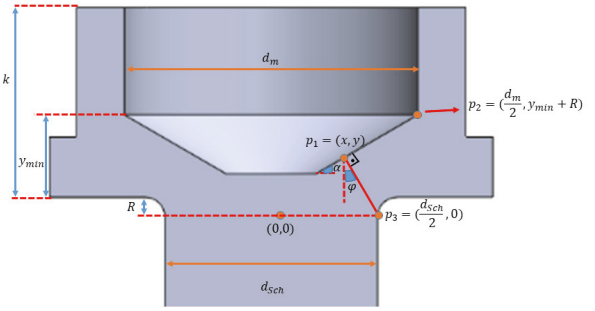

Fig. 3. Bolt cross section in the coordinate system.

- Then, the equation of the line l_2 is found by using the slope of the line, and the point $p_3 = (\frac{d_{Sch}}{2}, 0)$ in Eq. (4). The slope of the line l_2 can be found by using the fact that the slopes of perpendicular lines are opposite reciprocals, i.e., if the slopes of two perpendicular lines (l_1 and l_2) are multiplied, the value -1 is obtained.

$$y = -cot\,\alpha \,.\,(x - \frac{d_{Sch}}{2}) \tag{4}$$

- Finally, the intersection point, $p_1 = (x, y)$, of the lines l_1 and l_2 can be found by substituting Eq. (4) in Eq. (3) as follows:

$$-\cot\alpha \,.\left(x - \frac{d_{Sch}}{2}\right) = \tan\alpha \,.\left(x - \frac{d_m}{2}\right) + (y_{min} + R)$$

$$x.(\tan\alpha + \cot\alpha) = \frac{\cot\alpha.d_{Sch}}{2} + \frac{\tan\alpha.d_m}{2} - (y_{min} + R)$$

If $\tan\alpha = \frac{\sin\alpha}{\cos\alpha}$ and $\cot\alpha = \frac{\cos\alpha}{\sin\alpha}$ are substituted in the above equation, the x coordinate of the point p_1 is obtained. From now on, the equations $t = d_{Sch} + d_m$, $f = d_{Sch} - d_m$ and $y^* = y_{min} + R$ will be used to simplify notation, where d_m is the minimum socket diameter, d_{Sch} is the shaft diameter, R is the radius of the head, and y_{min} is the min residual floor thickness.

$$x = \frac{\cos\alpha^2.f - \sin 2\alpha.y^* + d_m}{2} \tag{5}$$

If x given in Eq. (5) is substituted into the equation of the line l_1, y coordinate of the point p_1 is obtained.

$$y = \frac{\tan\alpha}{2}.(\cos\alpha^2 f - \sin 2\alpha\,.\,y^*) + y^* \tag{6}$$

When the fracture pattern is rotated by 360 degrees around the shaft, the fracture cone is obtained (see Fig. 4). In order to find the minimum residual floor thickness, the maximum stress acting on the fracture cone in the head and the maximum tensile stress acting on the thread are compared. When the following condition is met, the head of the bolt assumed to satisfy the minimum ultimate tensile load defined in (ISO 898-1, 2004).

$$R_{mred}.A_{Sch} > R_m.A_S \tag{7}$$

where R_{mred} is the resultant of the tensile stress ($R_m.\sin\varphi$) and the shear stress ($\tau_B.\cos\varphi$), A_{Sch} is the surface area of the fracture cone formed in the head, R_m is the tensile stress acting on the thread and A_S is the nominal cross sectional area of the bolt thread (Fig. 2). The strength ratio of the bolts, x^*, is represented in the literature as $x^* = \frac{\tau_B}{R_m}$ and this coefficient varies according to the grade of the bolt given in (ISO 898-1, 2004). The total stress acting on the fracture cone is calculated as follows (Thomala and Kloos, 2007).

$$R_{mred} = \sqrt{(R_m.\sin\varphi)^2 + (\tau_B.\cos\varphi)^2} \tag{8}$$

By substituting $\tau_B = x^*.R_m$ into the Eq. (8), the following equation is obtained.

$$R_{mred} = R_m.\sqrt{\sin\varphi^2 + x^{*2}\cos\varphi^2} \tag{9}$$

If the fracture cone surface area given in Fig. 4(a), A_{Sch}, is cut straight along a certain fracture line to make it two-dimensional, a trapezoid is obtained. The resulting trapezoid is given in Fig. 4 (b).

When the values given in the formula of the trapezoid area are fulfilled, the following equation that calculates the surface area of the fracture cone is obtained:

$$A_{Sch} = \pi.(x + \frac{d_{Sch}}{2}).\frac{y}{\cos\varphi} \tag{10}$$

If x and y in Eq. (10) are substituted, the following equation is obtained:

$$A_{Sch} = \pi.(\frac{\cos\alpha^2.f - \sin 2\alpha.y^* + d_m}{2} + \frac{d_{Sch}}{2}).\frac{\frac{\tan\alpha}{2}.(\cos\alpha^2.f - \sin 2\alpha.y^*) + y^*}{\cos\varphi} \tag{11}$$

If Eq. (9) and (11) are substituted in Eq. (7), the following equation is obtained:

$$R_m.\sqrt{\sin\varphi^2 + x^{*2}\cos\varphi^2}\,.\pi.\left(\frac{\cos\alpha^2.f-\sin 2\alpha.y^*+d_m}{2}+\frac{d_{Sch}}{2}\right).\frac{\frac{\tan\alpha}{2}.(\cos\alpha^2.f-\sin 2\alpha.y^*)+y^*}{\cos\varphi} > R_m.A_S$$

The following equation is obtained after some simplifications:

$$(\cos\alpha^2\,.f-\sin 2\alpha\,.y^*+\mathrm{t}) > \frac{2.A_S.\cos\varphi}{\pi.\sqrt{\sin\varphi^2+x^{*2}\cos\varphi^2}.(\frac{\tan\alpha}{2}.(\cos\alpha^2.f-\sin 2\alpha.y^*)+y^*)} \quad (12)$$

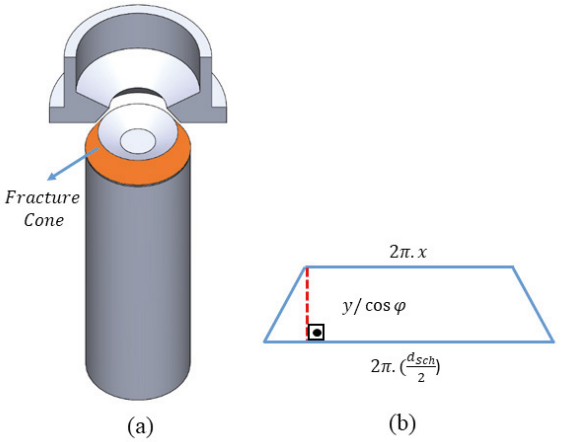

Fig. 4. (a) Schematic representation of fracture cone and (b) two-dimensional fracture cone surface area.

Here, if the dividend and denominator of the right-hand side of the Eq. (12) are simplified by taking parenthesis of $\frac{1}{x.\cos\varphi}$ on the right hand side of the equation, Eq. (13) is obtained:

$$(\cos\alpha^2\,.f-\sin 2\alpha\,.y^*+\mathrm{t}) > \frac{2.A_S}{x^*.\pi.\sqrt{(\frac{\tan\varphi}{x^*})^2+1}.(\frac{\tan\alpha}{2}.(\cos\alpha^2.f-\sin 2\alpha.y^*)+y^*)} \quad (13)$$

$$\tan\varphi = \frac{\frac{d_{Sch}}{2}-x}{\mathrm{y}} = \frac{\frac{d_{Sch}}{2}-\frac{\cos\alpha^2.f-\sin 2\alpha.y^*+d_m}{2}}{\frac{\tan\alpha}{2}.(\cos\alpha^2.f-\sin 2\alpha.y^*)+y^*} = \frac{\sin\alpha^2.f+\sin 2\alpha.y^*}{\sin\alpha.\cos\alpha.f+2\cos\alpha^2.y^*} \quad (14)$$

$\tan\varphi$ defined in Eq. (14) is substituted in Eq. (13) and the mathematical formula Eq. (15) is obtained after the mathematical operations such as cross-multiplication and square root.

$$y_{min} = \frac{-\sqrt{\frac{1}{\pi}.\cos\alpha^4(\pi.f^2-16.A_S.\sqrt{\frac{1-\cos\alpha^2}{x^{*2}.\cos\alpha^2-\cos\alpha^2+1}}+\pi.t^2+2.\pi.t.f)-\cos\alpha^2.f+2.\cos\alpha^4.f+\cos\alpha^2.t}}{4.\cos\alpha^3.\sin\alpha} - R \quad (15)$$

The resulting Eq. (15) also takes into account the radius of the head to shaft transition region to calculate the maximum socket depth. In order to test the model derived in Eq. (15), the sample specified in Section 2 was used with the following parameters: $d_{Sch} = 7.10$ mm; $d_m = 8.31$ mm; $R = 0.63$ mm; $x^* = 0{,}65$; $A_s = 36.60$. Socket diameter, d_m, was selected as the minimum diameter corresponding to N10 socket form.

3.2. Numerical modelling

Numerical analyses were carried out by using Simufact.forming software. Initially, a FE model was prepared based on the analytical formulation derived in the previous section. In this model, stresses were intended to be compared between head region and thread region, as compared in Eq. (8). To determine the critical socket depth, a linear and full-elastic model was created as shown in Fig. 5. Loading was applied by a rigid plate attached from the bottom of the bolt. Bolts were loaded in tension so that the stresses at the thread root or under head region reaches to around 640 MPa, the plastic deformation limit of 8.8 grade bolts as defined in (ISO 898-1, 2004). The critical socket depth was estimated for the case in which the stresses at the thread root and under head region were similar. The elastic constants, Elastic Modulus (E) and Poisson's ratio (ν), were taken as 210 GPa and 0.292, respectively. The element size of 0.5 mm for tetrahedral element type were used for numerical analysis. The numerical model used in this study was given in Fig. 5.

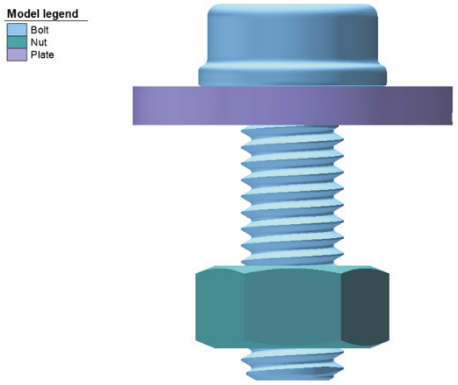

Fig. 5. FE Model to find y_{min}.

4. Results and discussion

Numerical analysis were repeated for different socket depths and the results were presented in Fig. 6. Effective (Von-Mises) stresses were compared at the thread region and at the fracture cone region to assess the crack initiation site i.e. failure location. Higher stresses were expected at the thread region for standard bolts, since failure from the thread implies that the design of the investigated bolt is suitable for the tested assembly conditions. Similar approach was employed in this study to assess the critical socket depth of the investigated bolt. For a detailed statistical study, 10 measurements were recorded from under head and thread root regions for the bolts with y values of 2.10 to 3.10 mm. The maximum, minimum and average effective stress results were plotted in Fig. 6. The rectangular boxes in the plots represents measurements falling in one standard deviation. Based on the effective stresses presented Fig. 6, stresses were observed to be higher at the thread region for the y values higher than 3.10 mm. Likewise, the stresses were higher at the head radius compared to thread region for the y values lower than 2.45 mm. According to FE modelling, the y_{min} was found as around 2,78 mm considering the box plots given in Fig. 6.

The y_{min} value of the investigated bolt was found as 2.82 mm and y value of point p_1 given in Fig. 3Fig. 3 was calculated as 2.33 mm by employing the analytical model developed in this study. The y_{min} value was found as around 2.78 mm from the numerical modelling. Analytical model estimated the socket depth on the safe side, i.e. socket depth value estimated by analytical model was higher compared to numerical modelling results. When analytical and FE modelling results were considered, the analytical model estimated the y_{min} value about 1.4% safer compared to FE modelling results. Therefore, the agreement between analytical and numerical modelling approaches can be considered as very good.

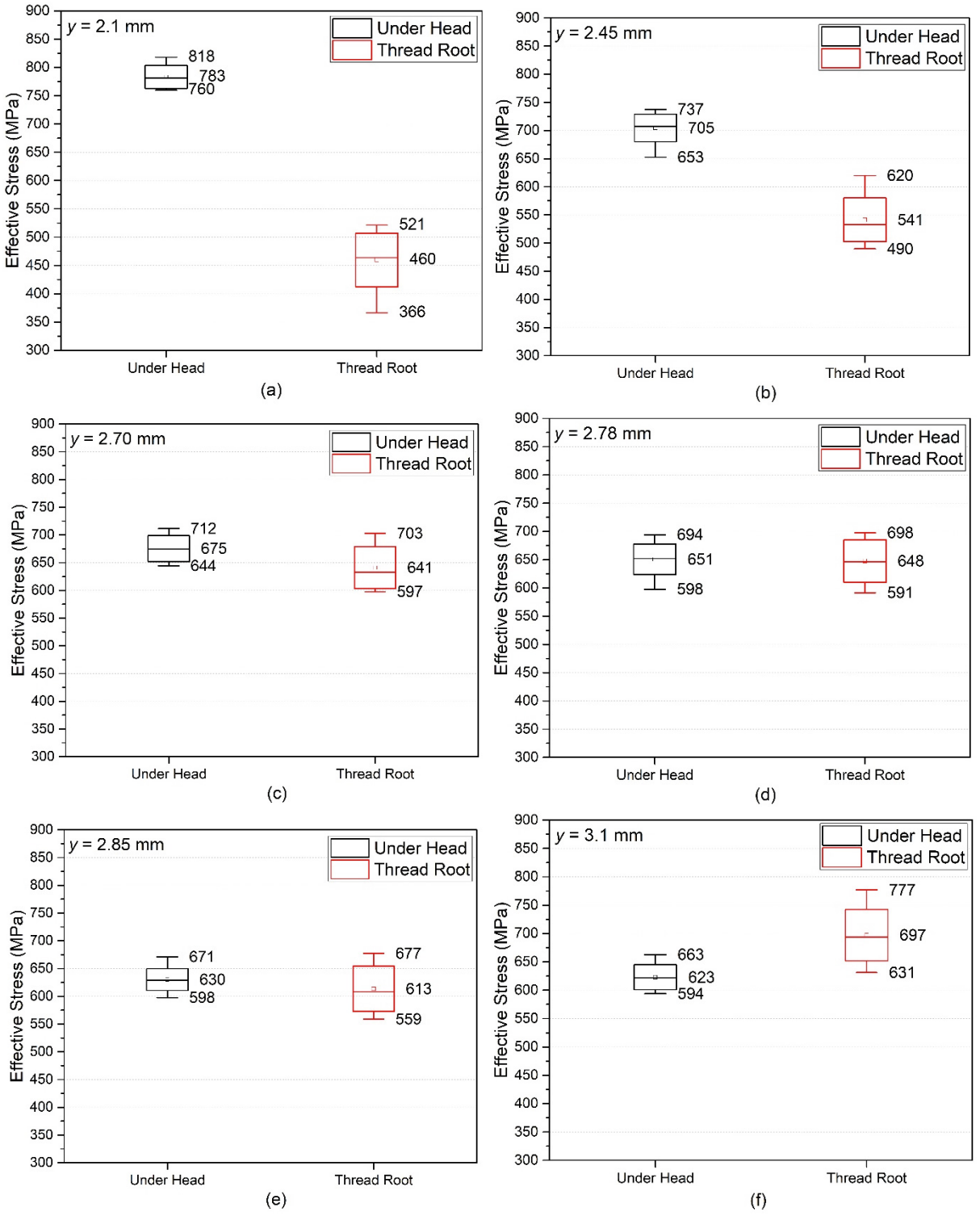

Fig. 6. Effective stress obtained from the under head and thread root region for bolts having y values (a) 2.10, (b) 2.45, (c) 2.70, (d) 2.78, (e) 2.85 and (f) 3.10.

5. Conclusions

In this study, an analytical model was developed to estimate maximum socket depth of the bolts having smaller shaft diameter than socket diameter. The results of the model were validated through FE modelling studies. The critical socket depth i.e. y_{min} value obtained by analytical model was 1.4% safer compared to numerical studies. Therefore, it can be concluded that the analytical model developed in this study can be used to estimate the critical socket depth of the bolts having shaft diameter smaller than socket diameter. Maximum weight reduction for the bolts having smaller shaft diameter than socket diameter can be achieved by increasing the socket depth i.e. decreasing the y value of the investigated bolt by using the analytical model developed in this study. Analytical model developed in the scope of this study will also be verified with experimental studies by producing cold forged bolts with various socket depths and conducting tensile test for these bolts.

References

Bickford, J., 1998. Handbook of Bolts and Bolted Joints, 1st ed, Handbook of Bolts and Bolted Joints. CRC Press, Boca Raton. https://doi.org/10.1201/9781482273786

Grimsmo, E.L., Aalberg, A., Langseth, M., Clausen, A.H., 2016. Failure modes of bolt and nut assemblies under tensile loading. J. Constr. Steel Res. 126, 15–25. https://doi.org/10.1016/j.jcsr.2016.06.023

Hedayat, A.A., Afzadi, E.A., Iranpour, A., 2017. Prediction of the Bolt Fracture in Shear Using Finite Element Method. Structures 12, 188–210. https://doi.org/10.1016/j.istruc.2017.09.005

Hongfei, G., Yan, J., Zhang, R., He, Z., Zhao, Z., Qu, T., Wan, M., Liu, J., Li, C., 2019. Failure Analysis on 42CrMo Steel Bolt Fracture. Adv. Mater. Sci. Eng. 2019, 1–8. https://doi.org/10.1155/2019/2382759

Hu, Y., Shen, L., Nie, S., Yang, B., Sha, W., 2016. FE simulation and experimental tests of high-strength structural bolts under tension. J. Constr. Steel Res. 126, 174–186. https://doi.org/10.1016/j.jcsr.2016.07.021

ISO 898-1, 2004. Mechanical Properties of Fasteners Made of Carbon Steel and Alloy Steel.

Novoselac, S., Kozak, D., Ergić, T., Damjanović, D., 2014. Fatigue damage assessment of bolted joint under different preload. Struct. Integr. Life 14, 93–109.

Pedersen, N.L., 2013. Overall bolt stress optimization. J. Strain Anal. Eng. Des. 48, 155–165. https://doi.org/10.1177/0309324712470233

Sorg, A., Utzinger, J., Seufert, B., Oechsner, M., 2017. Fatigue life estimation of screws under multiaxial loading using a local approach. Int. J. Fatigue 104, 43–51. https://doi.org/10.1016/j.ijfatigue.2017.06.034

Tanrıkulu, B., Toparli, M.B., Kılınçdemir, E., Yurtdaş, S., İnce, U., 2019. Determination of the critical socket depths of 10.9 and 8.8 grade M8 bolts with hexagonal socket form. Eng. Fail. Anal. 104, 568–577. https://doi.org/10.1016/j.engfailanal.2019.06.064

Tanrıkulu, B., Toparli, M.B., Kılınçdemir, E., Yurtdaş, S., İnce, U., 2018. Effect of socket depth on failure type of fasteners. Procedia Struct. Integr. 13, 1840–1844. https://doi.org/10.1016/j.prostr.2018.12.331

Thomala, W., Kloos, K.-H. (Eds.), 2007. Tragfähigkeit von Schraubenverbindungen bei mechanischer Beanspruchung, in: Schraubenverbindungen. Springer Berlin Heidelberg, Berlin, Heidelberg, pp. 135–208. https://doi.org/10.1007/978-3-540-68470-1_5